Chapter 7
Precise Orbit Determination of BeiDou Regional Navigation Satellite System Via Double-Difference Observations

Jun Zhu, Jiasong Wang, Guang Zeng, Jie Li and Junshou Chen

Abstract The precise orbit determination (POD) for BeiDou satellites mainly relies on a regional tracking network distributed in China area at the present time. The multi-satellite POD for BeiDou regional navigation satellite system via double-difference observations is presented. First, the double-difference phase measurements are modeled on ionosphere-free combination of B1 and B2 signals. The POD strategies are detailed, followed by a brief data-processing flow. Then, the POD tests based on regional network of domestic monitoring stations are developed, and the orbit quality assessed by arc overlaps and Satellite Laser Ranging (SLR) residuals shows an accuracy of about 20 cm in radial direction. Finally, contributions of the overseas monitoring stations to the POD accuracy of BeiDou satellites are investigated by introducing several IGS Multi-GNSS Experiment (IGS M-GEX) monitoring stations with BeiDou tracking capability into the multi-satellite POD test. The improved orbit accuracy indicates that more BeiDou observing sites should be established worldwide in future.

Keywords Precise orbit determination (POD) · BeiDou regional navigation satellite system · Double-difference observation · Multi-GNSS experiment (M-GEX)

Foundation item: National Natural Science Foundation of China (41274018).

J. Zhu (✉) · J. Wang
State Key Laboratory of Astronautic Dynamics, Xian 710043, China
e-mail: zhujun9306@126.com

J. Zhu · J. Wang · G. Zeng · J. Li · J. Chen
Xi'an Satellite Control Center, Xian 710043, China

J. Sun et al. (eds.), *China Satellite Navigation Conference (CSNC) 2013 Proceedings*, Lecture Notes in Electrical Engineering 245,
DOI: 10.1007/978-3-642-37407-4_7,

7.1 Introduction

The Compass/Beidou Navigation Satellite System is a global navigation satellite system (GNSS), which is independently developed, deployed, and operated by China. This system is still in progress, and is designed to provide global coverage around 2020. At present, only the Beidou regional navigation satellite system has been built up, which can provide coverage in the Asia–Pacific region with Positioning, Navigation, Timing (PNT), and short-message communication service capabilities [1, 2].

The PNT performance of GNSS is directly related to the satellite orbit accuracy. The precise orbit determination (POD) for BeiDou satellites can reach a radial accuracy of decimeter level currently, which is limited in tracking hour and geometric strength of regional configuration of ground-tracks observing in China area [3–5]. The POD performance can be improved by adopting some appropriate data processing techniques, such as differenced data processing. Differences of the original observations allow to eliminate or to reduce some biases, such as clock offset of satellites and receivers. The single-difference is simply defined as determining the relative differences between a pair of receivers measuring satellite simultaneously, and the double-difference means differencing between a pair of receivers and a pair of satellites [6].

In this paper a multi-satellite POD approach of processing double difference observations of phase and pseudorange observations for BeiDou regional navigation satellite system is presented, and the orbit accuracy assessment is performed by the overlapping difference and post fit of satellite laser ranging (SLR) residuals. In addition, to investigate the contribution of the configuration of ground-tracks geometry to the POD accuracy, measurements from several IGS Multi-GNSS Experiment (IGS M-GEX) monitoring stations with BeiDou tracking capability are processed. And some initially results are obtained.

7.2 Observation Modeling

The BeiDou satellites transmit navigation signals in Quadrature Phase-Shift Keying (QPSK) modulation on a total of three frequency bands (B1, B2, B3) [1, 7], which can form many high-quality combinations for navigation data process. Refer to paper [8], the Beidou pseudorange at high elevation can reach an accuracy of 20 $\sim$ 40 cm, and the accuracy of phase at high elevation is about 3 mm.

7.2.1 Double-Difference Observations Modeling

Beidou navigation system's original phase observations can be modeled as

$$\begin{aligned}\phi_r^s(t) = & f\rho(t_s,t_r)/c - f\delta t_s + f\delta t_r + \Delta\phi_{\text{trop}} - \Delta\phi_{\text{iono}} \\ & + \Delta\phi_{\text{rel}} + \Delta\phi_{\text{mult}} + N_r^s + \varepsilon(t)\end{aligned} \tag{7.1}$$

where, ϕ_r^s is the phase observation from satellite s to receiver r, t is the observation epoch, $f\,(=\text{B1},\ \text{B2},\ \text{B3})$ is the signal frequency, $\rho(t_s,t_r)$ is the geometric distance from satellite to receiver, c is velocity of light, δt_s is the satellite clock offset, δt_r is the receiver clock offset, $\Delta\phi_{\text{trop}}$ is tropospheric delay error, $\Delta\phi_{\text{iono}}$ is ionospheric delay error, $\Delta\phi_{\text{rel}}$ is relativistic effects error, $\Delta\phi_{\text{mult}}$ is multipath effects error, N_r^s is integer ambiguity, and $\varepsilon(t)$ is measurement noise.

The double-difference phase between stations and satellites is defined as the difference between satellites of the single-difference, and the single-difference can be got by 2 stations $(m,\ n)$ observing the same satellite in the same epoch. The double-difference phase is given by

$$\text{DD}(m,n,j,k) = (\phi_{mj} - \phi_{nj}) - (\phi_{mk} - \phi_{nk}) \tag{7.2}$$

The best feature of double-difference observation is the clock offset error was completely eliminated. Relativistic effects and multipath effects error also was significantly weakened. If the 2 stations in double-difference observation are close to each other, the tropospheric and ionospheric effects could be weakened. Substituting Eq. (7.1) into (7.2), we get

$$\begin{aligned}\text{DD}(m,n,j,k) = & f\left(\rho_m^j - \rho_n^j - \rho_m^k + \rho_n^k\right)/c + \left(\Delta\phi_{\text{trop}}^{mj} - \Delta\phi_{\text{trop}}^{nj} - \Delta\phi_{\text{trop}}^{mk} + \Delta\phi_{\text{trop}}^{nk}\right) \\ & - \left(\Delta\phi_{\text{iono}}^{mj} - \Delta\phi_{\text{iono}}^{nj} - \Delta\phi_{\text{iono}}^{mk} + \Delta\phi_{\text{iono}}^{nk}\right) + N_m^j - N_n^j - N_m^k + N_n^k + \text{dd}(\varepsilon)\end{aligned}$$

Where $\text{dd}(\varepsilon)$ is the measurement noise of combined observations. The noise's variance is magnified after combination, and the noise contains the residual multipath error.

7.2.2 Ionospheric-Free Combination

Ionospheric delay error is the maximum error in Beidou navigation system observation, if the clock offset error could be eliminated. It depends on the total electron content (TEC) in ionosphere. The first order term of ionospheric delay error is the main part, and can be eliminated by dual-frequency data combination, which is

$$\text{IF}(\phi_1,\phi_2) = \frac{1}{f_1^2 - f_2^2}\left(f_1^2\phi_1 - f_2^2\phi_2\right) \tag{7.3}$$

The second order term is only about 0.1 % of the first, and can be eliminated by triple-frequency data combination. That is

$$\begin{aligned} \mathrm{DIF}(\phi_1,\ \phi_2,\ \phi_3) &= \mathrm{IF}(\phi_1,\ \phi_2)\ -\ \mathrm{IF}(\phi_2,\ \phi_3) \\ &= \left(\frac{f_1^2}{f_1^2\ -\ f_2^2} - \frac{f_1^2}{f_1^2\ -\ f_3^2}\right)\cdot\phi_1\ -\ \left(\frac{f_2^2}{f_1^2\ -\ f_2^2}\right)\cdot\phi_2\ +\ \left(\frac{f_3^2}{f_1^2\ -\ f_3^2}\right)\phi_3 \end{aligned} \tag{7.4}$$

7.2.3 Tropospheric Delay Modelling

The zenith path delay (ZPD) due to tropospheric refraction is of the order of 2.3 m (or about 8 ns) for a station at sea level and standard atmospheric conditions, and can reach 20 m when elevation angle less than 10° [6]. Tropospheric delay contains two parts, the dry component and the wet component. We can calculate the tropospheric zenith delay by a priori model, and convert to the other directions using the mapping function. The dry component accounts for more than 90 % in tropospheric zenith delay. It could be almost completely corrected by using typical models, such as Hopfield model [9] or Saastamoinen model [10]. However, an uniform effective wet component correction model is difficult to build, due to the regional and seasonal changing characteristics of atmospheric humidity. In precise orbit determination, the wet component of tropospheric zenith delay is usually taken as a solve-for parameter in calculation. The whole tropospheric delay model can be written as

$$\Delta\rho_r^s(t,\ z)\ =\ \Delta\rho_{\mathrm{apr},\,k}\left(z_r^s\right)\ +\ \Delta\rho_k(t)f\left(z_r^s\right) \tag{7.5}$$

where, $\Delta\rho_r^s$ is the tropospheric path delay from receiver r to satellite s, z is the elevation of the observation scenario, $\Delta\rho_{\mathrm{apr},\,k}\left(z_r^s\right)$ is the slant delay according to an a priori model, $\Delta\rho_k(t)$ is the solve-for zenith path delay parameter, and $f\left(z_r^s\right)$ is the mapping function of $\Delta\rho_k(t)$.

7.2.4 Data Weighting

In satellite orbit determination, the numerical process method of code pseudorange and carrier phase measurements is weighting fusion. A typical prior weight is inversely proportional to measurement noise, and the measurement noise can be written as

$$\frac{\sigma_c}{\sigma_p}\ =\ 100 \tag{7.6}$$

where, σ_c is the measurement noise of code pseudorange, and σ_p is the measurement noise of carrier phase.

Table 7.1 System resulting data of standard experiment

Reference frame	
Station coordinate	ITRF2000 [15]
Data time tags	BDT
Solid tide	Wahr 1981 [16]
Ocean tide	GOT00 [12]
EOP	IERS C04
Precession/nutation	IAU2000 [17]
Planetary ephemeris	DE200
Gravity	JGM3 (12 × 12)
Satellite surface force and attitude	
Solar radiation	ECOM [13] + Box-Wing (pre-launch)
Thermo-radiation	Non-considered
Attitude	Nominal attitude
Data and parameterization	
Data using	Pseudorange and phase on frequency bands (B1, B2)
Data sampling and weighting	30s, elevation-dependent
Receiver and satellite clocks	Eliminated by double-differences
Troposphere model	Saastamoinen/Niell [14]
Antenna offset	Pre-launch
Phase windup	Wu (1993) [18]
Parameterization	Keplerian elements + CODE 9 parameters + ambiguities + zenith tropospheric delays

Observations at low elevations are generally much more susceptible to tropospheric refraction and multipath effects than those at high elevations. The unmodeled systematic errors decrease the quality of results. Using low-elevation observations, however, may also improve the estimation of tropospheric zenith delays and, consequently, the vertical component of station positions [11]. In order to optimize the use of low-elevation observations, there is an elevation-dependent weighting of observations, which is

$$w(\mathrm{z}) = \cos^2(\mathrm{z}) \tag{7.7}$$

7.3 POD Strategies

We apply the dynamic method to determine BeiDou satellites' orbit. The arc length is defined as 3 days. The ionospheric-free combination observations are used to form the double-difference observation equations. And the baselines are selected according to the criterion: the two stations have the maximum common-view satellites. The Least-Squares method is adopted for parameter estimation. The POD strategies are detailed in Table 7.1.

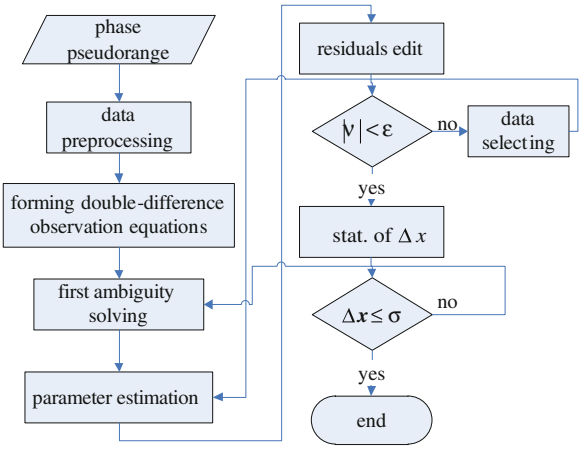

Fig. 7.1 A brief flow of data processing

A brief flow of data processing is showed as follows (Fig. 7.1).

7.4 POD Test Based on Regional Tracking Net

7.4.1 Overlapping Difference

A group of data from 07/17/2012 to 07/27/2012, domestic observation network data for 11 days, is selected for analysis. The orbit determination strategy is proposed in Part 3, determining a set of orbits with every 3 days observations (9 sets of orbits in total). So there is orbital overlap for 1 day between the set D the set D + 2. According to statistics orbit determination principle, the two sets of orbit, set D and D + 2, are mutually independence under ideal conditions. Therefore the consistency of the overlapping arcs orbits can be an index of the orbital accuracy in some way. Figure 7.2 shows the orbital overlapping differences of the Beidou operating satellites (C03, C05, C07, C10) in radial direction, and Fig. 7.3 shows the statistics of the three-dimensional orbital overlapping differences.

The results in Figs. 7.2 and 7.3 demonstrate the orbital differences in radial direction are about 20 cm, and about 1 m of three-dimensional position.

7.4.2 Independent SLR Residuals

Another method to estimate the precision of orbit determination is utilizing high-precision Satellite Laser Ranging (SLR) data for external checking on the results of the orbit determination. Independent SLR residuals directly reflect the precision

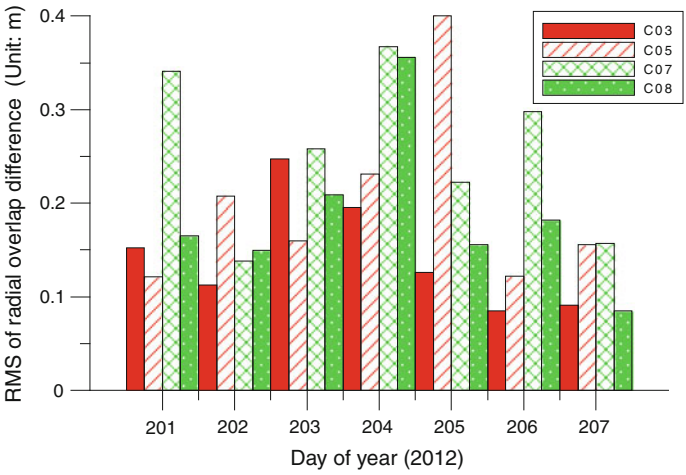

Fig. 7.2 Radial overlapping difference of BeiDou satellites

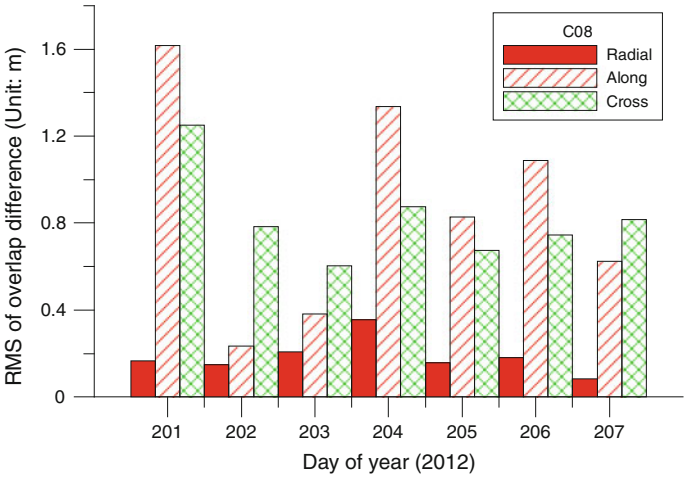

Fig. 7.3 Overlapping difference of BeiDou C08

of orbit determination. Supposing we get the SLR observation ρ_o at the time t, it can be expressed as

$$\Delta\rho = \rho_o - (\rho_c + \Delta\rho_{\text{stides}} + \Delta\rho_{\text{oloading}} + \Delta\rho_{\text{atm}} + \Delta\rho_{\text{rel}} + \Delta\rho_{\text{ec}} + \Delta\rho_{\text{st}} + \varepsilon \tag{7.8}$$

where, ρ_c is the distance from satellite to stations calculated by the POD results, $\Delta\rho_{\text{stides}}$ and $\Delta\rho_{\text{oloading}}$ are the influence of earth tides and sea tides to stations respectively, $\Delta\rho_{\text{atm}}$ is the atmospheric delay error which can be determined by

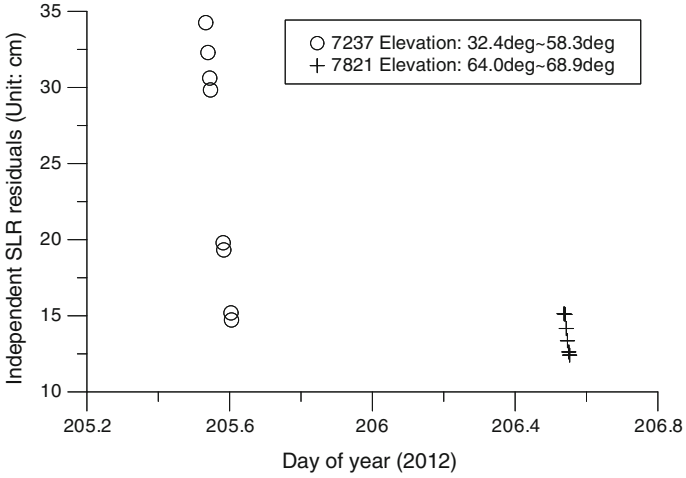

Fig. 7.4 Independent SLR residuals of BeiDou C08

Marini/Murray Model, $\Delta\rho_{rel}$ is the general relativity effects error, $\Delta\rho_{ec}$ and $\Delta\rho_{st}$ are the eccentric corrections and the displacement of observation stations respectively, ε is measurement error.

The SLR data we can get is relatively few. In the POD arcs mentioned in Part 4.1, we only have a small amount of data in July 23 (Station 7237) and July 24 (Station 7821). The post fit of SLR residuals were shown in Fig. 7.4. They indicate that the SLR residuals of Station 7821 are all less than 15 cm, while the SLR residuals of Station 7821 vary in 13 $\sim$ 35 cm. One possible reason is the elevation angles of Station 7821 are relatively lower.

7.5 IGS Multi-GNSS Experiment

In 2011, IGS initiated and organized an experiment utilize more than one navigation systems navigation, named IGS M-GEX. They tracked and monitored several GNSS signals at the same time in daily operations to analysis the performance and signal characteristics of the GNSS constellations emerging in recent years. Dozens of GNSS multimode tracking stations have been established in this experiment. Part of these stations can track Beidou Satellites, and they are shown in Table 7.2.

An analysis of Beidou satellite tracking data from these stations was presented in Ref. [8], and it preliminarily assessed the performance of Beidou regional navigation system. The results using orbit overlap method indicated that the precision of Beidou satellite orbits in three-dimensional position is 1 $\sim$ 10 m.

The M-GEX experiment provided valuable observations, which can be applied to study the influence of the layout of the station on the Beidou satellites POD

Table 7.2 M-GEX monitoring stations with BeiDou tracking capability

Name	Site	Lat	Long
CUT0	Bentley	−32.00	115.32
DLF1	Delft	51.59	4.23
KIR8	Kiruna	67.51	20.58
MAR7	Maartsbo	60.35	17.16
ONS1	Onsala	57.24	11.56
UNB3	Fredericton	45.57	293.21

precision. First, we analyzed the visibility of the satellite for tracking stations listed in Table 7.2. In the 6 stations listed in Table 7.2, all the stations except Station CUT0 are in the high latitudes. Actually, their tracking range for Beidou satellite is smaller, and there is low elevation observation data in almost all visible arcs. Figures 7.5 and 7.6 depicts the visibility of Beidou satellites to Station CUT0 and Station KIR8 for one day (Cut-off Elevation = 10°), respectively.

As illustrated in Fig. 7.5, the station CUT0 can observe two BeiDou GEOstationary (GEO) satellites (C03, C05), as well as all BeiDou Inclining Geostationary Synchronized Orbit (IGSO) satellites. Because it is located in southern hemisphere, this observing site should quietly enhance the geometric strength of the domestic regional tracking net. However, KIR8 has poor BeiDou tracking capability (Fig. 7.6). Almost no GEO satellite can be seen at this station. And most of the IGSO satellites are at low elevation. Obviously, measurements of KIR8 have limited contribution to POD of BeiDou satellites.

When integrating the observations obtained from M-GEX stations and observations from the domestic regional tracking net to carry out the POD test at the

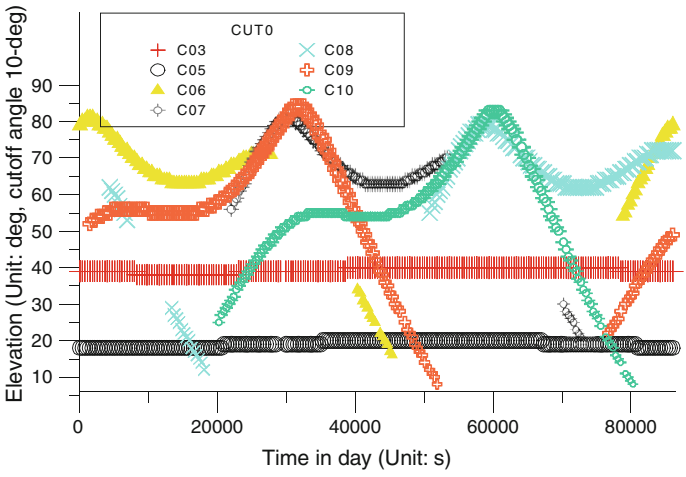

Fig. 7.5 Visibility of BeiDou satellites at station CUT0

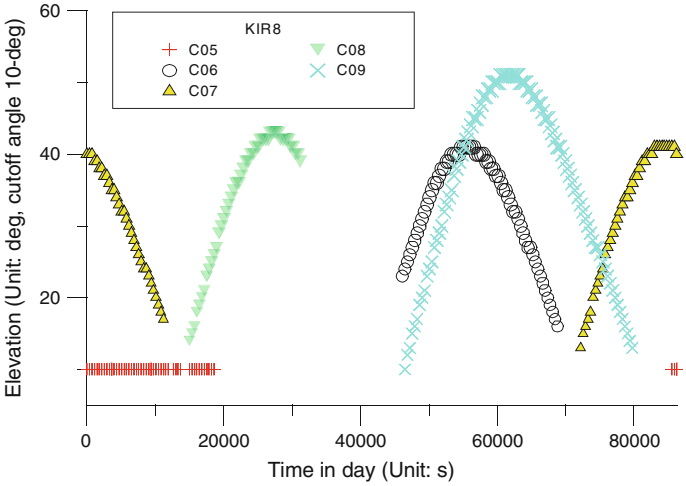

Fig. 7.6 Visibility of BeiDou satellites at station KIR8

same data period of time defined in Sect. 7.4, we can obtain a new result (Figs. 7.7 and 7.8).

In this two figures (Figs. 7.7 and 7.8), most of the radial overlapping differences of BeiDou satellites have decreased within 20 cm, and 3-D position differences have fall within 1 m, according to Figs. 7.2 and 7.3. As a result, though most of the IGS M-GEX monitoring stations have limited tracking capability for BeiDou satellites, they have improved the orbit accuracy a lot, compared to the orbit

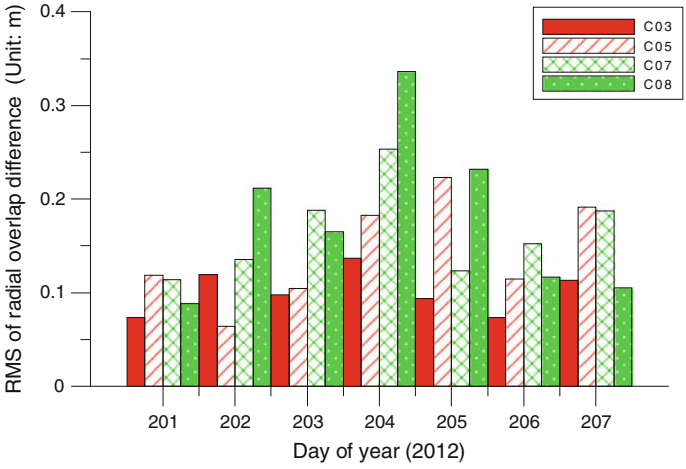

Fig. 7.7 Radial overlapping difference of BeiDou satellites, supported by IGS M-GEX monitoring stations

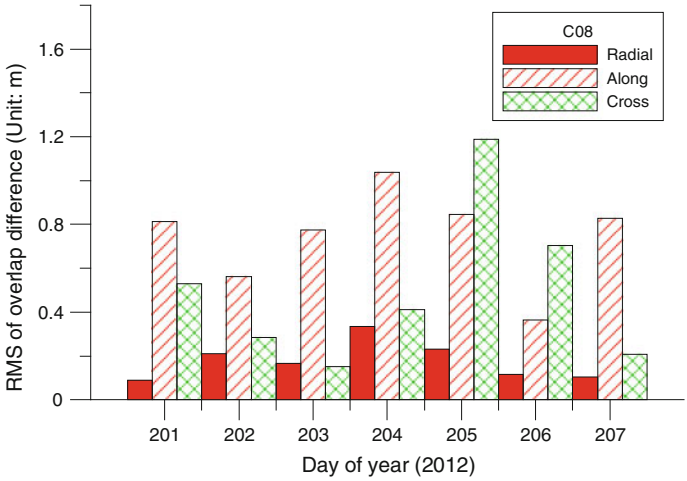

Fig. 7.8 Overlapping difference of BeiDou C08, supported by IGS M-GEX monitoring stations

derived from domestic tracking data only. The benefit of offshore monitoring stations is exhibited here preliminarily.

7.6 Summary and Conclusions

The multi-satellite POD for BeiDou regional navigation satellite system based on double-difference observation processing is discussed in this paper. Tests using overlapping differences and SLR residuals suggest the double-difference solutions of BeiDou regional ground-tracks net have achieved 20 cm radial accuracy, which can satisfy the needs of our domestic navigation users in the near future. With several IGS M-GEX monitoring stations observing BeiDou satellites supplied, the higher orbital accuracy can be obtained. Therefore, to improve the PNT service capability, it is of critical strategic significance to build up more BeiDou monitoring stations in the global region.

References

1. CSNO (2011) BeiDou navigation satellite system signal in space interface control document (Test Version), China satellite navigation office, December 2011. URL http://www.beidou.gov.cn/
2. Yang YX, Li JL, Xu JY et al (2011) Contribution of the compass satellite navigation system to global PNT users. Chinese Sci Bull 56(21):P1734–P1740
3. Wen Y, Liu Q, Zhu J et al (2007) The effect of TT and C deployment on the regional satellite navigation system, J Nat Univ Defense Technol, 29(1):P1–P6

4. Jianhua Z, LiuCheng C, XiaoGong H et al (2010) The precise orbit determination of GEO navigation satellite with multi-types observation, Scientia Sinica Phys.Mech and Astron, 40(5):P520–52
5. Geng T, Zhao Q (2009). Determining orbit of COMPASS-M1 Using international laser ranging data. Geomatics and information science of Wuhan University, 34(11):P1290–1292
6. Kaplan ED, Hegarty CJ (2006) Understanding GPS: principles and applications (Second edn). Norwood, MA 02062: ARTECH HOUSE
7. Han C, Yang Y, Cai Z (2011) BeiDou navigation satellite system and its timescales. Metrologia 48:P213–P218
8. Montenbruck O, Hauschild A, Steigenberger P et al (2012) Initial assessment of the COMPASS/BeiDou-2 regional navigation satellite system, Springer GPS Solut
9. Goad CC, Goodman L (1974) A modified hopfield tropospheric refraction correction model, In: Proceedings of the fall annual meeting of the american geophysical union, San Francisco, California, December 12–17
10. Saastamoinen II (1973) Contribution to the theory of atmospheric refraction[J]. Bulletin Geodesique 107:P13–P34
11. Meindl M, Schaer S, Hugentobler U et al (2004) Tropospheric gradient estimation at CODE: results from global solutions, in applications of GPS remote sensing to meteorology and related fields. J Meteor Soc Japan, 82(1B), P331–338, Meteorological Society of Japan
12. Ray RD (1999) A global ocean tide model from TOPEX/Poseidon altimetry: GOT99.2. NASA TM-1999-209478, NASA Goddard Space Flight Center, September
13. Springer TA, Beutler G, Rothacher M (1999) A new solar radiation pressure model for the GPS Satellites. GPS Solutions 3(2):P50–P62
14. Niell AE (1996) Global mapping functions for the atmosphere delay of radio wavelengths. J Geophys Res 101:P3227–P3246
15. Altamimi Z, Sillard P, Boucher C (2002) ITRF2000: A new release of the International Terrestrial Reference Frame for Earth science applications. J Geophys Res 107(B10):19
16. Wahr JM (1981) The forced nutation of an elliptical, rotating, elastic and oceanless Earth. Geophys J R astr Soc 64:705–727
17. McCarthy DD, Petit G (2004) IERS Conventions (2003) IERS Technical Note No. 32, 33–56
18. Wu JT, Wu C, Hajj GA, Bertiger WI, Lichten SM (1993) Effects of antenna orientation on GPS carrier phase. Manuscripta Geodaetica 18:91–98